Research Article

Multi-Objective Taguchi Optimization of Electrospinning Parameters for the Development of Poly-(vinyl alcohol)/Waste Wooden Utensil Nanocellulose/Phycocyanin Electrospun Fibers

Tabitha P. Vergel de Dios, Mia A. Luares, Will Arboleda, Myiesha Dane C. Calibara, John Ray C. Estrellado*

Department of Science, Technology, Engineering, and Mathematics, The Academy, De La Salle University – Laguna, Laguna Boulevard, LTI Spine Road, Barangays Biñan and Malamig, Biñan City, Laguna, 4024, Philippines

ABSTRACT

The lack of widespread commercial repurposing and recycling of waste wooden utensils contribute to pollution and toxic waste in the environment. This study aims to develop a sustainable method of repurposing waste wooden utensils into mechanically-robust electrospun fibers. Waste wooden utensil nanocellulose (WUNC) was produced using delignification, bleaching, and hydrolysis. Polymer mixtures consisting of 10% poly-vinyl alcohol (PVA), WUNC, and the pigment-protein complex phycocyanin (PC) were prepared for electrospinning following the Taguchi robust optimization design. Three parameters, namely WUNC addition (0.1, 0.2, 0.3 g./100 g), PC addition (0.1, 0.2, 0.3 g./100 g), and electrospinning voltage (25, 27.5, 30 kV), were varied to optimize loading capacity and tensile strength. Results showed WUNC addition of 0.2 g./100 g., PC addition of 0.3 g./100 g., and voltage of 25 kV optimal for loading capacity, with PC addition having the highest contribution at 44.54%. WUNC addition of 0.3 g./100 g., PC addition of 0.1 g./100 g., and voltage of 30 kV optimized tensile strength, with WUNC addition having the highest contribution at 57.99%. Produced WUNC resulted in a nanocellulose yield of approximately 16.81% with FTIR spectra revealing the removal of lignin and hemicellulose and increase of cellulose crystallinity. FTIR spectra for the electrospun fibers indicate successful integration of all components in the electrospun fibers. SEM analyses confirmed the creation of electrospun fibers within the nanosize range. Results confirmed the viability to extract nanocellulose and synthesize fibers from waste wooden utensils for enhancement of electrospun mats quality for biomedical applications, and offer new knowledge on wood-based nanomaterials.

Background

Annually, 80 billion pairs of chopsticks are manufactured in China alone (Oon, 2022). This excessive production of chopsticks leads to environmental issues, as waste wooden utensils fill up landfills. In attempts for sustainable repurposing, researchers and manufacturers use chopsticks as a source for different materials such as bio-oil (Chang et al., 2016), ethanol (Asada et al., 2011), and fuel (Chiang et al., 2012). Another study tackled the collection of cellulose nanofibrils from Aspen and Bode chopsticks (Suzuki et al., 2018). However, not many other researches cover this same scope. Given that chopsticks are rich and a potential source of cellulose, its applications and feasibility as a bio-based nanomaterial can simultaneously address these sustainability issues and this research gap.

Among the different nanomaterials, one of the most prominent is nanocellulose (Kaur et al., 2021). Researchers have extracted nanocellulose from various types of wood, including hardwoods like spruce and birch (Kumar et al., 2022; Raju et al., 2023; Muraleedharan et al., 2021) and processed woods like medium-density fiberboards (Couret et al., 2017). Some of the products that were produced with this extracted cellulose include reinforcement material, nanocarriers, films, and nanofibers. Waste-wood sources like chopsticks were also explored by Suzuki et al (2018) but with minimal application. Wood-derived nanocellulose is popular as a reproducible biomass resource from excess wood waste coming from housing, furniture, and businesses (Isogai, 2013). The produced product from wooden materials exhibits great qualities, such as high crystallinity, aspect ratio, Young's moduli, and tensile strength (Kargarzadeh et al., 2018).
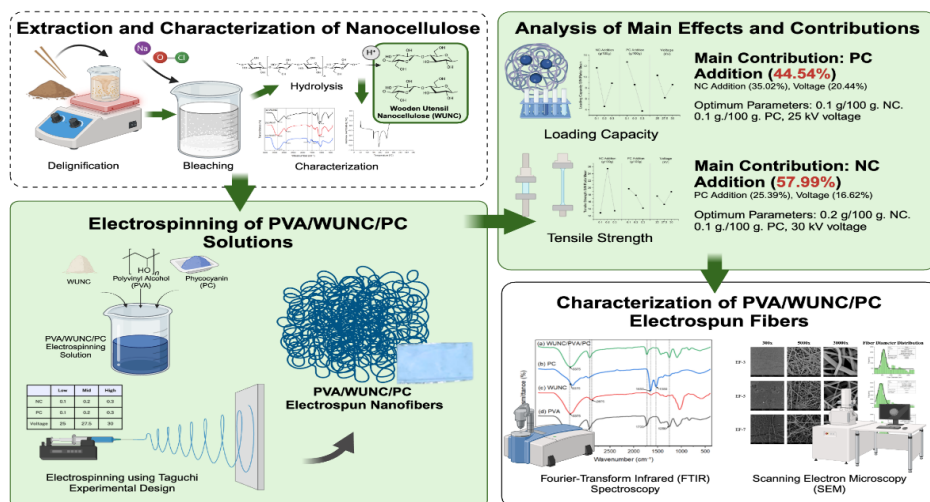
As a highly utilized bio-material, cellulose has been previously processed using solution casting into composite films (Xu et al., 2024) and Layer-by-Layer Assembly (LBL) into filter paper (Liao et al., 2024). Another emerging manufacturing technique is electrospinning into biomedical products (Ribeiro et al., 2021), which has the advantage of having precise control, more uniformity, and finer fibers compared to the previous methods. Additionally, it is cost-effective, versatile, and produces desired properties such as mechanical flexibility and high surface area (Gao et al., 2023). Electrospinning is defined as a process driven by an electro-hydrodynamic occurrence wherein a polymer solution is electrified and sprayed

through a syringe to form small fibers (Das et al., 2021). Previous studies often utilized electrospinning to produce nanocellulose reinforcement compounds and fabrics for sensors, displaying its flexible applications to many fields (Choi et al., 2021; Liao et al., 2011; Zhang et al., 2021). Over time, it has become the most frequent method for synthesizing nanofibers, particularly in biomedical applications (Chen et al., 2022). Typically, polymers such as poly(lactic acid), polyacrylonitrile, polyvinylidene fluoride, and polyvinyl alcohol (PVA) are added to further improve mechanical strength and ability to be spun in fibers (Patel et al., 2020; Xu et al., 2020; Wang et al., 2019; Wang et al., 2018).

To enhance its biomedical potential, pigments are often incorporated into fibers to improve biocompatibility, wound-healing, and other beneficial attributes. One study combined red pigments isolated from marine Bacterium Vibrio sp. to induce wound repair (Krishna et al., 2017). Another wound-healing pigment is phycocyanin which has been seen to have many beneficial effects to human skin, particularly antibacterial and antioxidant properties (Dranseikiene et al, 2022). Dranseikiene et al. (2022) further stated that phycocyanin was found to also have anti-inflammatory, anti-melanogenic, and anticancer properties. Additionally, Shanmugan et al (2017) observed the antibacterial activity of the extracted Phycocyanin from Oscillatoria sp. collected from dam water.

To assess the incorporation of additional polymers and pigments into nanofibers, loading efficiency and loading capacity are used to determine the percentage or amount of drug contained in the solution. Commonly used to measure drug loading, loading capacity refers to the amount of entrapped compound from the initial loading amount added (Trushina et al., 2022). Optimizing the loading capacity minimizes the loss of active compounds used in the product while maximizing the amount absorbed. In wound dressing applications, determining the loading capacity ensures that sufficient amounts of the pigment protein are present to bring proper wound healing effects. It is an essential property to optimize as it directly affects its efficacy and functionality.

Tensile strength testing is another common method of verifying the successful effect of adding polymers and checking the mechanical properties of nanofibers and wound dressings (Bülbül et al., 2022). This characteristic is one of the most important properties to be considered in assessing the effectiveness of these, as wound dressings that possess good tensile strength have the ability to withstand mechanical stresses. Wound dressings are subjected to frequent stress during movement, application, and removal, and must remain intact, as tearing can leave residue on wounds. High tensile strength is ideal as it increases durability of the dressings, allowing wounds to be properly protected. According to Bülbül et al. (2022), the ideal tensile strength of wound dressings range from 2.5 to 35 MPa.

Electrospun fibers generally exhibit weak mechanical properties (Pauly et al., 2016). PVA nanofibers with a lower degree of crystallization result in reduced mechanical strength (Lee et al., 2017). Previous studies have used cellulose nanocrystals to improve the mechanical properties of PVA electrospun fibers, including the study of (Wang et al., 2018), which indicated that increasing nanocellulose content initially enhanced tensile strength. However, no studies have tackled sourcing nanocellulose from waste materials. Thus, the PVA/WUNC/PC combination, particularly the addition of nanocellulose derived from waste wooden utensils, was employed to enhance the mechanical properties of electrospun fibers. Furthermore, this addition also aims to further improve the loading capacity of phycocyanin in PVA.

Previous studies have explored optimization methods such as the one-factor-at-a-time method (OFAT) and response surface methodology (RSM) to be utilized in electrospinning to optimize the integration of substances and parameters settings (Bösiger et al., 2018; Meng et al., 2015; Supaphol and Chuangchote 2008). While both these methods are viable in optimization, one-factor experimentation does not examine the interaction between parameters and is time-consuming (Zhang et al., 2021). On the other hand, Kandala et al. (2022) reported the Taguchi approach took 40% fewer runs than RSM when applied with the same experimental

design. The Taguchi method, a robust optimization method, requires fewer trials to achieve comparable results. Overall, Taguchi bears the advantages of streamline effect screening and inferring effects of factors with minimal runs.

Dr. Genichi Taguchi developed this optimization method to minimize the signal to noise ratio, or uncontrollable variables, using a systematic & statistical experimental design (Kim et al., 2004). By adjusting controlled variables prior to experimentation, this method improves testing quality and converts uncontrollable variables into desired characteristics. (Hamzaçebi, 2020). This method drastically reduces the amount of tests required to get the same results by utilizing orthogonal arrays (Li et al., 2019).

Only a few studies focus on the recycling and repurposing of waste wooden utensils, especially as a source of bio-based materials such as nanocellulose. Additionally, the effects and interactions of parameters that can affect the loading capacity and tensile strength within wound dressings are still unknown. This present study aims to explore these gaps by addressing the following research objectives:

- Extract nanocellulose from waste wooden utensils with the use of alkali treatment, bleaching, and acid hydrolysis
- Determine the yield on the produced nanocellulose and perform physicochemical characterization using Fourier Transform Infrared Spectroscopy (FTIR)
- Determine the contribution of wooden utensil nanocellulose (WUNC) addition, phycocyanin (PC) addition, and electrospinning voltage in the loading capacity and tensile strength of PVA/WUNC/PC electrospun fibers
- Optimize the solution and electrospinning parameters for the loading capacity and tensile strength of the PVA/WUNC/PC electrospun fibers using Taguchi optimization approach
- Characterize the produced electrospun fibers using FTIR and Scanning Electron Microscopy (SEM)

Scope and Limitations

This research only utilized chopsticks from a single local restaurant and excluded samples from different restaurants and types of chopsticks. Furthermore, this study only investigated the feasibility of extracting cellulose from chopsticks while not optimizing the yield. During optimization, only the factors electrospinning voltage, nanocellulose addition, and phycocyanin addition were considered but do not explore other factors such as humidity, flow rate, or nozzle diameter which could influence fiber properties. While the research focuses on mechanical and chemical properties, real-world application testing such as biodegradability and cytotoxicity are beyond the scope of the study.

Significance of the Study

This study aims to explore the viability of chopsticks as a source for nanocellulose extraction and its further applications in the biomedical field. The findings of this study will be valuable to researchers as an alternative source of nanocellulose, a popular material for sustainable material synthesis and reinforcements. Meanwhile, this study can also be significant for the medical field and sustainability efforts as the produced materials have wound-healing capabilities and opens a new method of repurposing waste. While previous researchers have studied the extraction of nanocellulose from chopsticks, there is a gap in exploring its application. By identifying the optimal parameters for the production of fibers and integration of beneficial substances, this study contributes to the evolving efforts of sustainable transitioning.

Methods
Materials

Waste bamboo chopsticks were collected from a local restaurant located in Santa Rosa, Laguna. The waste chopsticks were disinfected through a series of soaking in boiling water and cleaning with dishwashing liquid. Waste bamboo chopsticks were dried using a Thermo Scientific Lindberg/Blue rapid drying oven (Thermo Fisher Scientific, Massachusetts, United States), and pulverized using Panasonic MX-AC210S mixer grinder (Panasonic Corporation, Osaka, Japan). The pulverized waste bamboo chopsticks were passed through a 60-mesh screen for uniform particle distribution.

Chemicals

Chemicals used in the extraction of nanocellulose were sodium hydroxide pellets (Loba Chemie Pvt. Ltd., Mumbai, India) for delignification, sodium hypochlorite (Dalkem Corporation, Quezon City, Philippines) for bleaching, and concentrated sulfuric acid (J.T. Baker, New Jersey, United States) for acid hydrolysis. The polymers used for the electrospinning solutions were partially hydrolyzed poly-vinyl alcohol BP-24 (Chang Chun Petrochemical Co. Ltd., Taipei, Taiwan) and phycocyanin (Xi'an Qinghekang Biotechnology Co., Shaanxi, China).

Equipment

The equipment used for the extraction of nanocellulose were a hot plate with magnetic stirrer (Torrey Pines Scientific Inc., California, United States) and Scientz 18-N Freeze Dryer (Ningbo Scientz Biotechnology Co., Ltd., Zhejiang, China). Inovenso NS1 NanoSpinner Electrospinning Device (Inovenso Ltd., Istanbul, Turkey) located in Philippine Nuclear Research Institute (PNRI) was used for electrospinning. Characterization was done using the Shimadzu UV-1700 Spectrophotometer (Shimadzu Corporation, Kyoto, Japan) for loading capacity, Shimadzu IRSpirit (Shimadzu Corporation, Kyoto, Japan) for FTIR, Zwick Roell Z0.5 Universal Testing Machine (Zwick Roell Group, Ulm, Germany) for tensile strength, and JEOL JSM 5310 Scanning Electron Microscope (JEOL Ltd., Tokyo, Japan) located in I-Nano Research Facility, Sta. Ana, Manila for morphological analysis.

Experimental Phases

The phases of the experiment are shown in Figure 1. The first phase involves the extraction of wasted wooden utensil-derived nanocellulose (WUNC), as well as its characterization. The second phase includes the preparation of the electrospinning solutions using the polyvinyl alcohol (PVA), phycocyanin (PC), and the extracted WUNC, while the third phase involves the electrospinning of the solutions. The fourth phase focuses on the optimization of the tensile strength and loading capacity of the produced electrospun fibers. The fifth and final phase includes the FTIR and SEM characterization of the PVA/WUNC/PC fibers.
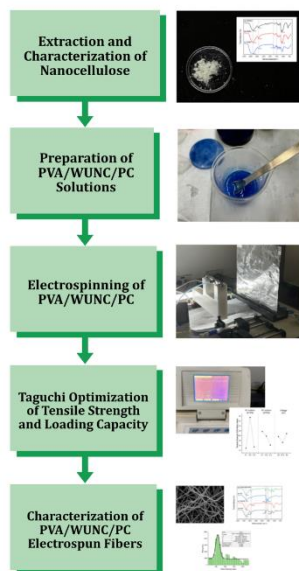
Figure 1. Experimental phases for the Taguchi optimization of electrospinning parameters of PVA/WUNC/PC fibers.

Experimental Design

The experimental design followed in this study is the Taguchi Optimization Design. The design uses Taguchi optimization in multiple electrospinning studies such as the L16 orthogonal array design to optimize 5 factors like voltage and polymeric solution addition to reduce experimentation runs from 1024 to 16 (Mo-

hammadi et al. 2020). Most similar to the L9 orthogonal array, this Taguchi design combines three factors (PC addition, NC addition, electrospinning voltage) of three levels to minimize the experimentation of the inefficient full-factorial design: from $3^3 = 27$ experiments to nine experiments (Abbas et al., 2018).

Described in Table 1 are the parameter values that will be referenced with the Taguchi optimization methods. Nanocellulose and phycocyanin addition both have low values of 0.1 g./100 g., mid values of 0.2 g./100 g., and 0.3 g./100 g. On the other hand, spinning voltage has a low value of 25 kV, mid value of 27.5 kV, and high value of 30 kV.

Table 1. Parameter levels for the Taguchi robust optimization design of experiment

Parameters	Low (-1)	Mid (0)	High (1)
NC Addition (g./100 g.)	0.1	0.2	0.3
PC Addition (g./100 g.)	0.1	0.2	0.3
Spinning Voltage (kV)	25	27.5	30

Table 2. Taguchi orthogonal array for the optimization of preparation parameters for maximum loading capacity (mg. phycocyanin/g. fiber) and tensile strength (MPa)

Run No.	NC Addition (g./100 g.)	PC Addition (g./100 g.)	Voltage (kV)	Loading Capacity (mg/g)	Tensile Strength (MPa)
EF-1	-1	-1	-1	y_{11}	y_{21}
EF-2	-1	0	0	y_{12}	y_{22}
EF-3	-1	1	1	y_{13}	y_{23}
EF-4	0	-1	0	y_{14}	y_{24}
EF-5	0	0	1	y_{15}	y_{25}
EF-6	0	1	-1	y_{16}	y_{26}
EF-7	1	-1	1	y_{17}	y_{27}
EF-8	1	0	-1	y_{18}	y_{28}
EF-9	1	1	0	y_{19}	y_{29}

The preparation of PVA/WUNC/PC solutions for electrospinning involved combining a prepared PVA solution at with varying WUNC addition, PC addition, and electrospinning voltage at 3 levels, Low (-1), Mid (0), and High (1) as shown in Table 1. WUNC addition and PC addition are measured per 100 g of PVA added. Other variables were kept controlled including PVA concentration at 10%, PVA amount at 20 g, and Electrospinning Flow Rate at 1 mL/h.

The combination of parameters in Table 2 will be used to determine the optimal dependent values, loading capacity and tensile strength. Furthermore, the values from Table 1 were used as inputs for the independent

variables or parameters. Taguchi's orthogonal array approach utilizes the combinations of factors or parameters with different levels or different values of the parameters to achieve efficiency. This array reduces the time, costs, errors made in the process, and improves the understanding of the cause and effect relationship between factors and the product

Extraction of Wooden Utensil-derived Nanocellulose (WUNC)

This method adapts methods from the study of Couret et al. (2017) with few modifications. Pulverized chopsticks underwent alkali treatment with 4% NaOH for 2 hours. Lignin

acts as a binder for wood components, and its removal is essential to isolate cellulose. This process ensures total delignification of the wood samples. Afterwards, the delignified cellulose was neutralized and freeze-dried to prepare for the following processes.

After the extraction of cellulose, the samples were bleached using 2.5% v/v sodium hypochlorite (NaOCl) and then freeze-dried once more. "The samples were then bleached twice with NaOH and subjected to acid hydrolysis using 50% v/v sulfuric acid (H_2SO_4) at 50 °C for two hours, following Suzuki et al. (2018) and Singh et al. (2023)."
.

Characterization of Wooden Utensil-derived Nanocellulose (WUNC)

As one of the steps of characterization, the determination of percent yield assesses the efficiency of the extraction methods by comparing the mass of the processed material from the original material. This evaluation compares previous extraction methods and viability of the material to be scaled to commercial purposes. Additionally, FTIR characterization would be performed on the extracted material to determine the different functional groups present in the nanocellulose. This allows the observation of changes in chemical structure from chopsticks, to cellulose, to nanocellulose, ensuring the complete removal of lignin and hemicellulose.

Thermal behavior of the nanocellulose was monitored in accordance with the protocol of Velasquéz et al. (2022) and Huang et al. (2017). DSC 25 differential scanning calorimeter (TA Instruments, Delaware, United States) was used to observe the thermal behavior of the nanocellulose sample with mass of 5 mg. from 50°C to 500°C with a heating rate of 10°C/min. The thermogram of the nanocellulose was used to analyze the endothermic and exothermic peaks signifying the initial melting stage and crystallization stage.

Preparation of PVA/WUNC/PC Electrospinning Solutions

A 10% w/w poly-(vinyl alcohol) (PVA) solution was first prepared using 20 g. of PVA and 200 mL of distilled water. The distilled water was heated, maintaining a temperature of around 70-80 °C on a hotplate with a magnetic stirrer. Stable temperature was maintained by slowly stirring PVA granules until it had finally dissolved. After cooling, the electrospinning solutions were mixed with different concentrations of nanocellulose and phycocyanin into PVA solution, according to the generated Taguchi design of the experiment.

Electrospinning of PVA/WUNC/PC Solution

The experiment setup of the electrospinning device, processing the PVA/WUNC/PC polymer solution into nanofibers is shown in Figure 2. The electrospinning phase of this research will be conducted in the Philippine Nuclear Research Institute (PNRI), using Inovenso NS1 NanoSpinner Electrospinning Device. The electrospinning setup was prepared by loading the PVA/WUNC/PC solutions into the syringe pump. The silicone tubing was connected to the nozzle. Aluminum foil was placed on the collector plate for the collection of the electrospun fibers.
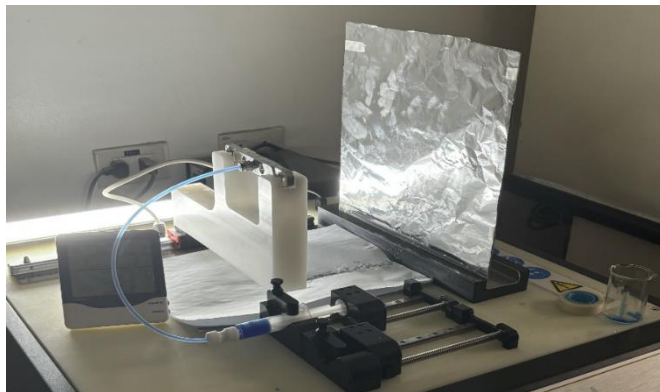

Figure 2. Experimental setup of the electrospinning process of PVA/WUNC/PC electrospinning solutions

During the electrospinning process, by adopting the methods of Ji et al. (2021), with slight modification based on initial trials, the following parameters will be varied: WUNC addition, spinning voltage, and PC addition following similar methods to the L9 Taguchi array. The solutions were electrospun at 29.5 °C for 1 hour and were placed in a dry box to to eliminate moisture.

Determination of Loading Capacity

Loading capacity tests would be performed to measure the amount of incorporated phycocyanin (PC) into the electrospun fibers. The concentration of phycocyanin in the electrospun fibers will be calculated using the formula in Equation 1. Absorbance values at 615 nm and 652 nm (A_{615} and A_{652}) will be measured using UV–Vis spectroscopy. This method follows Irmak (2020), who cited the original formula from Bennett and Bogorad (1973), as shown in Equation 1.

$$PC \left(\frac{mg}{mL}\right) = \frac{A_{615} - 0.474 * A_{652}}{5.34} \qquad \text{(Eq. 1)}$$

Wherein:
PC is the concentration of phycocyanin in mg/mL
A_{615} is the absorbance at 615 nm
A_{652} is the absorbance at 652 nm

The loading capacity will then be determined using Equation 2 below, following the study of Khandual et al. (2021).

$$LC \left(\frac{mg}{g}\right) = \frac{PC * V_s}{m_f} \qquad \text{(Eq. 2)}$$

Wherein:
LC is the loading capacity in mg./g.
V_s is volume of solution in mL
m_f is the mass electrospun fibers in g.

Determination of Tensile Strength

To test the mechanical properties of the electrospun nanofibers, tensile strength was tested using the Zwick Roell Universal Testing Machine. The parameters for the testing are as follows: 25 mm grip to grip separation at starting point, 500 mm/min speed start position, 0.1 N pre-load, 10 mm/min speed pre-load, 12.5 mm/min position controlled test speed, and a force shutdown threshold at 50 N. This characterization is crucial to determine the wearability and durability of the nanoscaled fibers for future applications.

Determination of Signal-to-Noise (SN) Ratio

After obtaining the data from Taguchi optimization methods, the signal-to-noise ratio was calculated using Equation 3 to determine the effect of each parameter in producing the optimal electrospun fiber. Fraley et al., (2023) highlights the process of calculating the signal and noise values to derive their ratio in their paper and following formula. Specifically, this method would be utilizing the larger-the-better SN to maximize the response or output, which would be loading capacity and tensile strength in this study (Karazi et al., 2019).

$$SN_i = 10 \log\left(\frac{\bar{y_i}^2}{s^2}\right) \qquad \text{(Eq. 3)}$$

Wherein:
SN_i is the signal-to-noise ratio
$(\bar{y_i})^2$ is the signal power
s^2 is the noise power

The percent contribution formula shown in Equation 4 was also used to determine the contribution of each factor into the respective response variable, which was then ranked in comparison with the other parameters.

$$\% \, C_x = \frac{SS_x}{\sum SS} * 100\% \qquad \text{(Eq. 4)}$$

Wherein:
%C_x is the percent contribution of parameter x
SS_x is the sum of squares of parameter x
$\sum SS$ is the summation of all sum of squares

Characterization of PVA/WUNC/PC Electrospun Fibers
Fourier-Transform Infrared Spectroscopy (FTIR)

FTIR was conducted to confirm successful delignification and investigate the internal structure and morphology of the PVA/WUNC/PC fibers after these respective objectives. Similar to methods by Singh et al. (2023) and Sihag et al., (2022), the FTIR spectra were recorded in the range of wavenumbers 500–4000 cm−1 using the Shimadzu IRSpirit infrared spectrometer. The FTIR spectrum of the individual materials would also be recorded to review the interactions and verification of integration into one solution.

Scanning Electron Microscopy (SEM)

To obtain clear images of the morphology, such as beading and weaving, of the electrospun fibers, SEM was employed at three different magnifications: 300x, 5000x, 30000x, using the JEOL JSM 5310 Scanning Electron Microscope. This imaging characterization follows the examples of Chandra et al., (2016) in accordance with established protocols from related studies. GIFT macro on ImageJ was used to create the fiber diameter distribution. The parameters for the fiber diameter scanning are as follows: 45 degrees of rotation, 8 line length, 100 bin size, 190px to 10000 nm (manually measured from the scale on the 5000x zoom SEM micrograph), and 1024 pixel crop. Percentage thresholds were manually to adjusted to maximize the inclusion of measurable fibers.

Ethics Statement

Pursuant to the University's Code of Research Ethics and Guide to Responsible Conduct of Research, Operational Guidelines for the Research Ethics Review Committee, and the DLSU-IS SHS Research Manual, the researchers created a Material Safety Data Sheet (MSDS) of the chemicals involved in the study, used proper personal protective equipment to ensure safety, performed proper handling and storage of all equipment and chemicals involved in the study, and reported all results of the experiments with honesty, transparency, and accurac

Results and Discussion
Extraction of Nanocellulose

Shown in Figure 3 are the steps for extraction: (a) pulverized chopsticks, (b) bleached cellulose, (c) bleached nanocellulose. The extraction process involved initial mechanical pulverization of the chopsticks, followed by delignification, acid hydrolysis, and bleaching, resulting in the products shown in Figure 3.
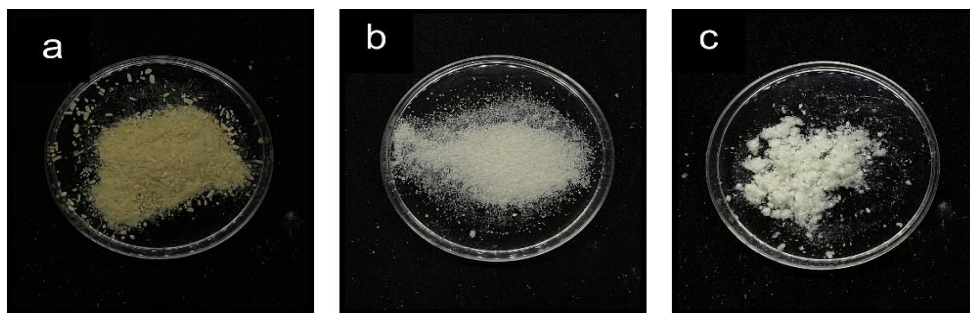

Figure 3. Extraction process of nanocellulose from (a) pulverized wooden chopsticks (CHST), (b) wooden utensil cellulose (WUC), and (c) wooden utensil nanocellulose (WUNC)

As shown in Figure 3, the appearance of the pulverized chopsticks initially appeared brown in color. After the delignification process, the cellulose turned into a lighter shade, as lignin is a significant contributor of color (Zhang et al., 2020). Bleaching was repeatedly performed to further lighten the cellulose. Subsequently, acid hydrolysis was performed to extract nanocellulose. This resulted in a darker coloration, as parameters including the temperature, acid concentration, and the duration of hydrolysis affected the process. As reported by Lin et al. (2019), high temperatures, strong acid concentrations, and extended hydrolysis durations contribute to nanocellulose darkening.

$$\% Y_n = \frac{m_n}{m_s} * 100\% \qquad \text{(Eq. 5)}$$

Wherein:

%Y_n is the percent yield of nanocellulose

m_n is the mass of nanocellulose produced

m_s is the mass of initial sample (ground chopsticks)

The mass changes after each processing step is outlined in Table 3. The mass changes after each processing step is outlined in Table 3. After delignification, bleaching, and acid hydrolysis, 20.00 ± 0.00 g of pulverized chopsticks achieved 3.53 ± 0.84 g of nanocellulose, resulting in a percent yield of 17.65 ± 4.2%.

Table 3. Mass of wooden utensil and its weight post-delignification, post-bleaching, and post-hydrolysis

Extraction Stage	Bone Dry Mass (g.)	Mass Loss (g.)	Percent Mass Loss (%)
Wooden Utensil	20.00 ± 0.00	-	-
Post-Delignification	14.68 ± 1.96	5.32 ± 1.96	26.60 ± 9.80
Post-Bleaching	6.80 ± 1.42	7.88 ± 0.56	53.98 ± 3.75
Post-Hydrolysis	3.53 ± 0.84	3.27 ± 0.64	48.21 ± 3.04

After delignification, the percent yield was calculated using Equation 5 (Vishnoi et al., 2023). The 26.60 ± 9.80% mass was loss during the conversion due to the removal of lignin, hemicellulose, and other impurities. After the bleaching process, the mass was significantly reduced by 53.98 ± 3.75%, as this also removes non-cellulosic components and causes severe oxidation when higher concentrations of bleach is used (Wang & Zhao, 2020). Furthermore, the mass loss of 48.21 ± 3.04% post-hydrolysis is due to the breakdown of amorphous regions in the cellulose, and the formation of nanocellulose from crystalline regions.

Characterization of Extracted Nanocellulose

FTIR spectroscopy is crucial in analyzing the extracted nanocellulose by monitoring the chemical composition and present functional groups. For chemical composition analysis, it confirms the removal of non-cellulosic material therefore validating the methods of this study (Wahib et al., 2022). This was achieved by analyzing the presence or absence of specific peaks, which correspond to distinct functional groups. Additionally, FTIR analysis helps ensure that no chemical defects or unwanted residues were introduced during the extraction process.

Summarized in Table 4 are the findings taken from the FTIR spectrum. Specifically, it lists down the functional groups that were observed along with its respective wavenumber.

Fourier Transform Infrared Spectroscopy (FTIR) analysis identified the different functional groups present in nanocellulose (WUNC), cellulose (WUC), and chopsticks (CHST), as shown in Figure 4. The FTIR spectra of WUNC, WUC, and CHST showed peaks at 3375 cm-1 which correspond to O-H stretching, indicating the presence of hydroxyl groups (Sihag et al., 2022; Singh et al., 2023; Sulaiman et al., 2011; Wulandari et al., 2016). The peaks for WUNC and WUC at 2875 cm-1 and 1125 cm-1 correspond to C-H stretching (Chieng et al., 2017; Wulandari et al., 2016) and C-O-C stretching (Zarina & Ahmad, 2014; Wulandari et al., 2016), respectively.
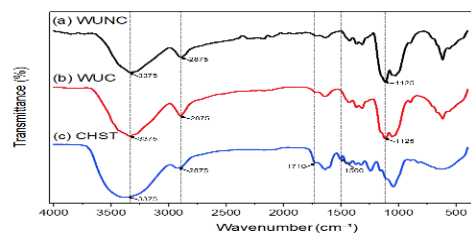

Figure 4. Fourier-transform infrared (FTIR) spectra of (a) wooden utensil nanocellulose (WUNC), (b) wooden utensil cellulose (WUC), and (c) wooden chopsticks (CHST)

Table 4. Wavenumbers and corresponding functional groups of chopsticks, cellulose, and nanocellulose

Substance	Wavenumber (cm^{-1})	Functional Group
Nanocellulose (WUNC)	3375	O-H stretch (Sihag et al., 2022; Singh et al., 2023)
	2875	C-H stretch (Chieng et al., 2017)
	1125	C-O-C stretch (Zarina & Ahmad, 2014)
Cellulose (WUC)	3375	O-H stretch (Wulandari et al., 2016)
	2875	C-H stretch (Wulandari et al., 2016)
	1125	C-O-C stretch (Wulandari et al., 2016)
Chopsticks (CHST)	3375	O-H stretch (Sulaiman et al., 2011)
	2875	CH$_2$ stretch (Sulaiman et al., 2011)
	1710	C=O stretch (Jelle et al., 2012)
	1500	C=C stretch (Jelle et al., 2012)

The thermal behavior of nanocellulose is key to understanding the crystalline behavior of the nanocellulose extracted from wooden utensils. Aside from the spectral analysis, thermal behavior was also observed using differential scanning calorimetry. The DSC curve of the extracted nanocellulose is shown in Figure 5.
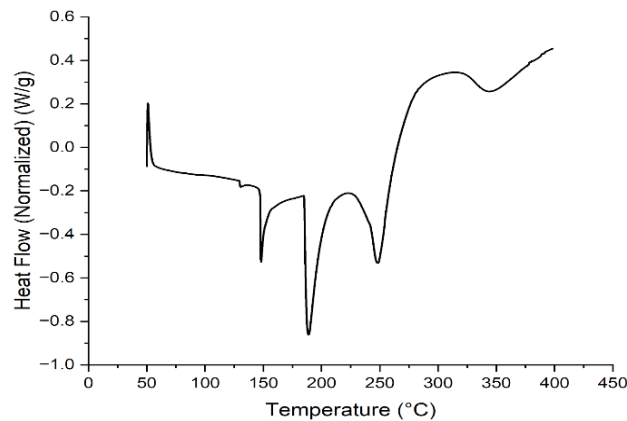

Figure 5. Differential scanning calorimetry (DSC) curve of wooden utensil nanocellulose (WUNC)

In Figure 5, the evolution of bound moisture happens within the range of 50°C - 132.81°C, where residual moisture is removed from the nanocellulose matrix (Charoensopa et al., 2024). The nanocellulose matrix exhibits a high surface area with hydroxyl (-OH) groups, as shown in the FTIR spectra in Figure 4, which facilitates the retention of moisture on the nanocellulose surface (Kondor et al., 2021). The presence of amorphous regions in the nanocellulose was observed in the endothermic peak at 148°C, indicating presence of hemicellulosic components in the nanocellulose sample (Charoensopa et al., 2024). Moreover, the onset of thermal degradation is observed at around 248.77°C, indicating the cleavage of glycosidic bonds in cellulose. Huang et al. (2017) reported an instance of onset decrease by 80°C in the thermal degradation of nanocellulose due to the replacement of hydroxyl groups with sulfated groups during sulfuric acid hydrolysis, with an initial degradation onset at 348.45°C for unhydrolyzed cellulose. However, a similar endothermic peak was also observed in this study, indicating that there is residual unhydrolyzed cellulose still present in the nanocellulose sample. In summary, the study has successfully produced nanocellulose, but further characterization of crystallinity is important to further optimize the production of cellulose nanocrystals.

.Wound dressings must be able to sustain their shape and form when exposed to constant body heat and even in situations where body temperature rises, such as fever. Normal body temperature ranges from 36.1°C - 37.2°C, rising up to 41°C if

experiencing fever (Gefen, 2021). As shown in Figure 5, losses of moisture only occur in ranges far beyond the expected body temperature, indicating that the produced fibers would serve well as a wound dressing.

Electrospinning of PVA/WUNC/PC Solution Mix

During the electrospinning process, the fibers were formed due to the coulombic differences of the nozzle and collector plate (Haider et al., 2018). Electrospun fibers are formed as the solvent evaporates that creates a steady stream of fiber deposition at the collector plate (Garcia et al., 2022). Representative areas of the nine electrospun PVA/WUNC/PC fibers with variations being attributed to the differences in parameters are collaged in Figure 6.
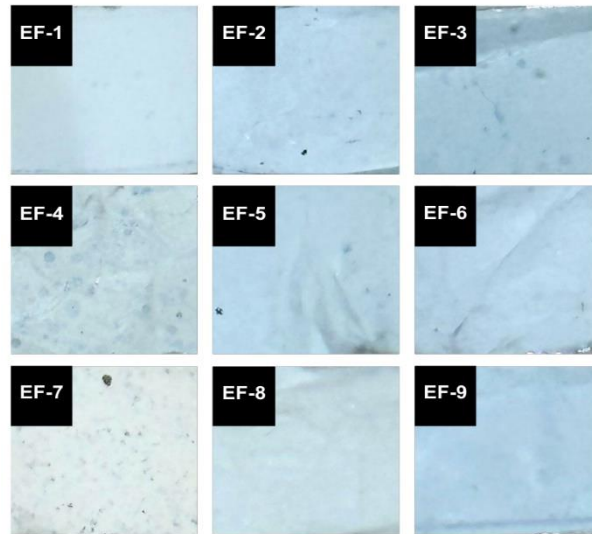

Figure 6. Electrospun fibers produced using Taguchi design of experiment

While some runs such as EF-1 and EF-8 exhibited uniform surface morphology, the other runs displayed varying smoothness and irregularities such as wrinkles and dispersions. EF-3, EF-5, and EF-6 strongly display wrinkling, which may be due to buckling instability during electrospinning (Pai et al., 2009). EF-3, EF-4, AND EF-7 have particularly distinct particle dispersions, as simple blending electrospinning may cause uneven distribution of drugs in fibers (Sun et al., 2019). The fibers also have a range of colors spanning from white-gray to light blue due to the different amounts of PC addition similar to the slight blue-green PC/chlorophyll nanofibers produced by Martin et al. (2023).

Loading Capacity

The results of loading capacity optimization given the following combination of parameters in each run are shown in Table 5.

Table 5. Loading capacity of PVA/WUNC/PC fibers

Run No.	Nanocellulose Addition (g./100 g.)	PC addition (g./100 g.)	Voltage (kV)	Loading Capacity, Mean ± SD (mg/g)	Confidence Interval ($\alpha=0.05$)
EF-1	0.1	0.1	25	35.89 ± 3.43	(32.01, 39.78)
EF-2	0.1	0.2	27.5	4.39 ± 1.11	(3.13, 5.64)
EF-3	0.1	0.3	30	63.83 ± 46.77	(10.9, 116.75)
EF-4	0.2	0.1	27.5	2.68 ± 2.07	(0.33, 5.02)
EF-5	0.2	0.2	30	23.85 ± 10.08	(12.44, 35.26)
EF-6	0.2	0.3	25	75.44 ± 46.73	(22.56, 128.32)

Run No.	Nanocellulose Addition (g./100 g.)	PC addition (g./100 g.)	Voltage (kV)	Loading Capacity, Mean ± SD (mg/g)	Confidence Interval (α=0.05)
EF-7	0.3	0.1	30	13.44 ± 2.21	(10.94, 15.95)
EF-8	0.3	0.2	25	27.47 ± 13.09	(12.66, 42.28)
EF-9	0.3	0.3	27.5	35.04 ± 20.92	(11.37, 58.72)

As revealed in Table 5, there is significant loading capacity with the highest being 75.44 mg/g, resulting from parameters of WUNC addition of 0.2 g./100 g., PC addition of 0.3 g./100 g., and voltage of 25 kV. In contrast, the lowest capacity of 2.68mg/g had parameters of WUNC addition of 0.2 g./100 g., PC addition of 0.1 g./100 g., and voltage of 27.5 kV. These results align with the findings of Luraghi et al. (2021), which stated the optimal electrospinning voltage was between 15-25 kV to ensure uniform fiber formation and therefore more favorable surfaces for loading. Higher voltages (>25 kV) can lead to thinner fibers, which may improve drug dispersion but also risk drug loss due to jet instability. These results also followed the pattern of higher additive substance concentrations resulting in better loading. In the same study, Luraghi et al. (2021) stated that higher polymer concentration increases viscosity, which improves drug entrapment or loading within the fiber matrix.

The calculations to get the loading capacity signal-to-noise ratio for each run are displayed in Table 6. To solve for the SN ratio, you would divide the found signal value by the noise value according to the formula by Fraylet et al. (2023).

The calculated Signal-to-Noise ratios for swelling capacity per parameter and parameter level are shown in Table 7. Below these calculated values are the mean Signal-to-Noise ratio, as well as its rank in contribution and its percent contribution.

Table 6. Loading capacity signal-to-noise ratio calculations

Run No.	Loading Capacity Mean (mg/g)	Signal ($\bar{y}_i^2$)	Noise (s_i^2)	Signal-to-Noise Ratio
EF-1	35.89	1288.41	11.77	20.39
EF-2	4.39	19.24	1.00	11.93
EF-3	63.83	4073.70	2187.42	2.70
EF-4	2.68	7.16	4.30	2.21
EF-5	23.85	568.99	101.67	7.48
EF-6	75.44	5691.51	2183.83	4.16
EF-7	13.44	180.67	4.90	15.67
EF-8	27.47	754.69	171.27	6.44
EF-9	35.04	1228.13	437.61	4.48

Table 7. Loading capacity Taguchi optimization signal-to-noise results

Parameter Level	NC Addition (g./100 g.)	PC Addition (g./100 g.)	Voltage (kV)
1	11.68	12.76	10.33
2	4.62	8.62	6.21
3	8.86	3.78	8.62
Signal to Noise	7.06	8.98	4.12
Rank	2	1	3
% Contribution	35.02%	44.54%	20.44%

Shown in Figure 7 is the main effects plot for loading capacity. It can be inferred from the graph that PC addition has the highest contribution to the loading capacity of the

electrospun fibers, as indicated by the steep slopes across its level. An inverse relationship between PC addition and loading capacity was also observed. The second most significant effect on loading capacity is NC addition, as evidenced by the steep and varied slopes across its levels. However, there is no linear relationship between NC addition and loading capacity.

Voltage had the least significant effect, as indicated by the relatively flat slope in its plot. Similar to NC addition, there is no linear relationship between voltage and loading capacity. The best combination of parameters for the highest signal-to-noise ratio is 0.1 g./100 g. NC addition, 0.1 g./100 g. PC addition, and 25 kV voltage.
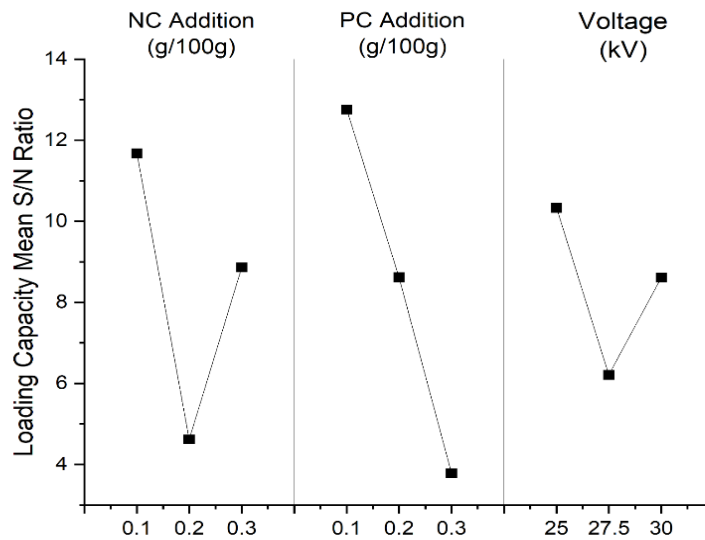

Figure 7. Main effects plot for loading capacity

Using the formula presented in Equation 3, the analysis of Taguchi's robust optimization methods revealed the parameters that most contributed to the optimal results of loading capacity. Phycocyanin (PC) addition exhibited the highest signal-to-noise (S/N) ratio at 8.98, making it the most influential parameter, followed by WUNC addition, then electrospinning voltage. Voltage had the least effect, with an S/N ratio of 4.12. These findings are consistent

with Luraghi et al. (2021) who reported that voltage had a moderate influence on the drug loading and polymer or additive substance concentration had a high influence.

Tensile Strength

The results of tensile strength optimization given the following combination of parameters in each run is shown in Table 8.

Table 8. Tensile strength of PVA/WUNC/PC fibers

Run No.	Nanocellulose Addition (g./100 g.)	PC addition (g./100 g.)	Voltage (kV)	Tensile Strength Mean (MPa) ± SD (mg/g)	Confidence Interval (α=0.05)
EF-1	0.1	0.1	25	2.63 ± 0.25	(2.34, 2.92)
EF-2	0.1	0.2	27.5	2.61 ± 0.85	(1.64, 3.57)
EF-3	0.1	0.3	30	2.52 ± 0.94	(1.46, 3.58)
EF-4	0.2	0.1	27.5	6.03 ± 0.42	(5.55, 6.5)
EF-5	0.2	0.2	30	5.02 ± 0.12	(4.89, 5.16)
EF-6	0.2	0.3	25	3.97 ± 0.35	(3.57, 4.37)
EF-7	0.3	0.1	30	6.24 ± 1.02	(5.09, 7.4)
EF-8	0.3	0.2	25	5.30 ± 1.39	(3.72, 6.88)
EF-9	0.3	0.3	27.5	5.09 ± 1.14	(3.81, 6.38)

The mean tensile strength of the different samples of electrospun fibers can be found in Table 8. The highest recorded tensile strength result was 6.24 MPa, followed by 6.03 MPa, and 5.30 MPa. The values in the middle range were 5.09 MPa, 5.02 MPa, and 3.97 MPa. The lowest values were 2.63 MPa, 2.61 MPa, and 2.52 MPa. The trial with the highest tensile strength had the following parameters: WUNC addition of 0.3 g./100 g., PC addition of 0.1 g./100 g., and voltage of 30 kV. The trial with the lowest tensile strength, on the other hand, had the following parameters: WUNC addition of 0.1 g./100 g., PC addition of 0.3 g./100 g., and voltage of 30 kV. Across multiple trials, tensile strength tended to increase alongside the incorporation of nanocellulose, with the 3 runs containing 0.1 g./100 g. WUNC addition having the lowest among the 9 runs. This observation aligns with Paulett et al. (2017), who reported that, which states that increasing the concentration of nanocellulose strengthens the electrospun fibers. However, going over a specific threshold leads to a decrease in tensile strength.

Displayed in Table 9 are the calculations to get the tensile strength signal-to-noise ratio for each run. The S/N ratio was calculated by dividing the signal by the noise, following the formula by Fraylet et al. (2023). The calculated Signal-to-Noise ratios for Tensile strength per parameter and parameter level are shown in Table 10. Below these calculated values are the mean Signal-to-Noise ratio, as well as its rank in contribution and its percent contribution.

Table 9. Tensile strength signal-to-noise ratio calculations

Run No.	Tensile Strength Mean (MPa)	Signal ($\bar{y}_i^2$)	Noise (s_i^2)	Signal-to-Noise Ratio
EF-1	2.63	6.92	0.06	20.36
EF-2	2.61	6.79	0.73	9.68
EF-3	2.52	6.37	0.88	8.60
EF-4	6.03	36.32	0.18	23.14
EF-5	5.02	25.23	0.01	32.37
EF-6	3.97	15.79	0.13	21.01
EF-7	6.24	38.98	1.04	15.73
EF-8	5.30	28.09	1.94	11.61
EF-9	5.09	25.94	1.30	13.02

Table 10. Tensile strength Taguchi optimization signal-to-noise results

Parameter Level	NC Addition (g./100 g.)	PC Addition (g./100 g.)	Voltage (kV)
1	12.88	19.74	17.66
2	25.51	17.89	15.28
3	13.45	14.21	18.90
Signal to Noise	12.63	5.53	3.62
Rank	1	2	3
% Contribution	57.99%	25.39%	16.62%

Shown in Figure 8 is the main effects plot for tensile strength. The variable with the most significant effect on tensile strength is NC addition, as indicated by the steep slopes across levels. However, no linear relationship could be observed. The variable with the second most significant effect is PC addition. A negative correlation was observed between the addition of PC and tensile strength. The variable with the least significant effect is voltage. Like NC addition, voltage exhibited a non-linear effect with tensile strength. The best combination of parameters for the highest signal-to-noise ratio is 0.2 g./100 g. NC addition, 0.1 g./100 g. PC addition, and 30 kV voltage.

The signal-to-noise (S/N) ratio formula was applied to assess the contribution of the three parameters on the tensile strength of the

electrospun fibers. The signal-to-noise ratio of the different parameters are shown in Table 10. The most significant factor was the WUNC addition, with a signal-to-noise ratio of 12.63. This further supports the role of nanocellulose integration as a key factor in increasing tensile strength of electrospun fibers (Leones et al, 2021). This was followed by PC addition, with a signal-to-noise ratio of 5.53. The factor with the least significant effect on tensile strength was voltage, with a signal-to-noise ratio of 3.62. These results align with the study of Hajieghrary et al. (2024) which states that cellulose nanofibers play a significant role in affecting the tensile strength of electrospun materials. O'Connor et al. (2021) reported that applied voltage does not significantly affect the mechanical properties of electrospun fibers.

Morphological Characterization of PVA/WUNC/PC Electrospun Fibers
FTIR Characterization of PVA/WUNC/PC Electrospun Fibers

FTIR analysis was conducted to identify the different functional groups present in poly-vinyl alcohol (PVA), phycocyanin (PC), wooden utensil nanocellulose (WUNC), and electrospun fiber sample (PVA/WUNC/PC), as shown in Figure 9. The summary of key wavenumbers taken from the PVA/WUNC/PC Solution FTIR spectrum is shown in Table 11. Common functional groups identified in the spectra of the components were highlighted and the interactions on these wavenumbers were also discussed.
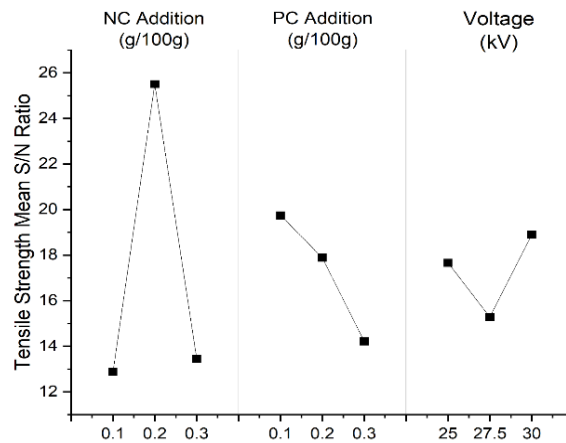

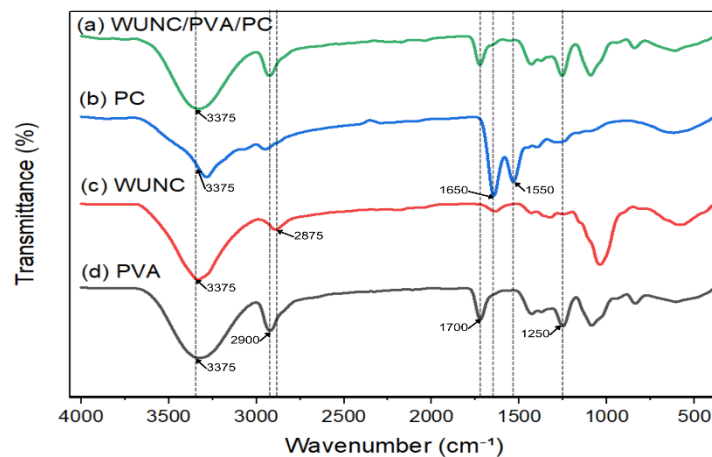Figure 8. Main effects plot for tensile strength

Figure 9. FTIR spectra of (a) PVA/WUNC/PC electrospun fibers, (b) phycocyanin (PC), (c) wooden utensil nanocellulose (WUNC), and (d) poly-(vinyl alcohol) (PVA)

Table 11. Wavenumbers and corresponding functional groups of PVA/WUNC/PC solution and components

Substance	Wavenumber (cm⁻¹)	Functional Group
PVA/WUNC/PC	3375	O-H stretch (Kharazmi et al., 2015)
	2900	CH_2 asymmetric stretch (Kharazmi et al., 2015)
	1700	C=O carbonyl stretch (Kharazmi et al., 2015)
	1250	C-H bend (Kharazmi et al., 2015)
PC	3375	O-H and N-H stretch (Zhang et al., 2017)
	1650	C=O stretch (Buliga et al., 2024)
	1550	N-H bend (Buliga et al., 2024)
WUNC	3375	O-H stretch (Sihag et al., 2022; Singh et al., 2023)
	2875	C-H stretch (Chieng et al., 2017)
	1125	C-O-C stretch (Zarina & Ahmad, 2014)
PVA	3375	O-H stretch (Kharazmi et al., 2015)
	2900	CH_2 asymmetric stretch (Kharazmi et al., 2015)
	1700	C=O carbonyl stretch (Kharazmi et al., 2015)
	1250	C-H bend (Kharazmi et al., 2015)

All samples showed broad peaks at 3375 cm-1 which corresponds to O-H stretching and indicates the presence of hydroxyl groups (Kharazmi et al., 2015; Sihag et al., 2022; Singh et al., 2023; Zhang et al., 2017). The peaks for PC at 1650 cm-1 and 1550 cm-1 correspond to the C=O stretching of Amide I and N-H bending of Amide II bands, respectively (Buliga et al., 2024) which were not seen in the (PVA/WUNC/PC) solution due to the low amount of PC and weakening of the amide bands. The peak seen at around 2875 cm-1 and 1125 cm-1 in WUNC is assigned to C-H stretching (Chieng et al., 2017) and C-O-C stretching of cellulose and hemicelluloses (Zarina & Ahmad, 2014), respectively. The peaks for PVA at around 2900 cm-1, 1700 cm-1, 1250 cm-1, and 1000 cm-1 correspond to CH2 asymmetric stretch, C=O carbonyl stretch, C-H bend, and C-O stretch, respectively (Kharazmi et al., 2015). The similarity of the IR spectra of PVA and (PVA/WUNC/PC) could be attributed to the high concentration of PVA in the solution.

SEM Characterization of PVA/WUNC/PC Electrospun Fibers

Scanning Electron Microscopy (SEM) was performed to analyze the morphology of three samples of electrospun fibers, EF-3, EF-5, and EF-7, as well as its relation to their mechanical properties. Additionally, the distribution of fiber diameter was identified to further understand the morphological characteristics of the fibers.
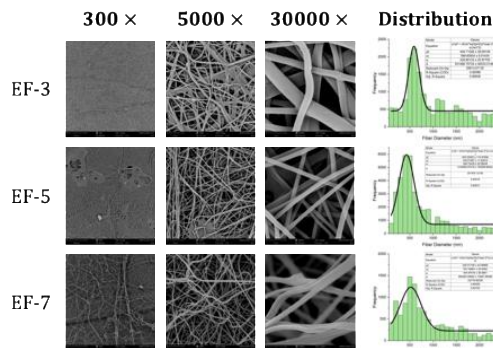

Figure 10. SEM imaging of electrospun fibers produced using 0.1 g./100 g. NC addition, 0.3 g./100 g. PC addition, and 30 kV voltage (EF-3); 0.2 g./100 g. NC addition, 0.2 g./100 g. PC addition, and 30 kV voltage (EF-5); and 0.3 g./100 g. NC addition, 0.1 g./100 g. PC addition, and 30 kV voltage (EF-7) at 300x, 5000x, and 30000x magnification

The micrographs confirm the successful formation of fibers from the electrospinning fibers. Beading from the electrospinning polymer can be seen especially in EF-5 and EF-7 indicating imperfections from the electrospinning process. Histograms fitted with Gaussian curves for the fiber diameter distribution also revealed the mean and standard deviation of the fibers. The fiber diameter distribution was collected from the 5000x magnifications of the 3 electrospun fibers. Manually set percent pixel thresholds for the GIFT macro ImageJ fiber distribution are 20, 30, and 19, respectively. The mean ± standard deviation for EF-3, EF-5, EF-7 was revealed to be 589.61 ± 229.80 nm, 430.01 ± 326.73 nm, and 521.05 ± 444.98 nm, respectively. This confirms the successful spinning of fibers into the nano range of 1-1000 nanometers (Valizadeh & Mussa Farkhani, 2014).

The images reveal highly porous structures for EF-7 and EF-5, while EF-3 shows less porosity. In a previous study by Jiyas et al. (2023), lower porosity of fibers resulted in higher tensile strength. However, the opposite could be observed for EF-7, EF-5, and EF-3, which were revealed to have tensile strengths of 6.24 ± 1.02 MPa, 5.02 ± 0.12 MPa, and 2.52 ± 0.94 MPa, respectively. This could be due to the diameter distribution of the fibers which are shown in Figure 10. EF-7 was revealed to have the most even distribution, followed by EF-5, and EF-3. Loading capacities of EF-7, EF-5, and EF-3 correspond to 13.44 ± 2.21 mg/g, 23.85 ± 10.08 mg/g, and 63.83 ± 46.77 mg/g, respectively. This could be due to the beading seen in EF-7 and EF-5. Meanwhile, EF-3 was seen to have the smoothest fiber structure, leading to higher loading capacity.The produced electrospun fibers show that phycocyanin was successful as an additional component in electrospinning as an antioxidative agent without disruption to the morphological characteristics of the fibers, as compared to the work of Gul and Cano (2021), which utilized PVA/NC electrospun fibers and had similar SEM results

Conclusions

This study demonstrated the feasibility of extracting nanocellulose from waste wooden utensils, specifically from discarded chopsticks, establishing them as a viable source. FTIR analysis identified functional groups present in the different samples. These results confirm successful and clean extraction of the nanocellulose from the waste wood and the effect of the different polymer components onto the electrospun fiber. The prepared PVA/WUNC/PC solution also exhibited successful electrospinnability through the production of nanofibers. FTIR also indicated potential viability in biomedical applications due to enhanced mechanical properties with biomedical properties due to the addition of phycocyanin. The tensile strength of electrospun fibers increased with nanocellulose incorporation, reaching a maximum of 6.24 MPa and the lowest strength of 2.52 MPa. Signal-to-noise calculations also ranked the influence of the electrospinning parameters to loading capacity to PC addition, WUNC addition, and then voltage from most to least significant. SEM micrographs confirmed the successful formation of nanofibers from the electrospinning process, while mean fiber diameters of 589.61 nm, 430.01 nm, and 521.05 nm validated their nanoscale dimensions. The addition of phycocyanin into the electrospinning process was successful and did not have any negative morphological impacts on the electrospun fibers. The results also open up room for optimization of other parameters relevant for wound dressing production which would improve the viability of the product as a wound dressing. Future work is recommended to include swelling ratio tests, which reflects the fiber's ability to manage wound exudate, cytotoxicity tests, which ensures the material is non-toxic to human cells, and antioxidant tests, which evaluates the antioxidant activity of the fibers. Furthermore, this also prompts future research to synthesize and test a commercially applicable wound dressing made from this study's produced PVA/WUNC/PC nanofibers.

References

Abbas, J. A., Said, I. A., Mohamed, M. A., Yasin, S. A., Ali, Z. A., & Ahmed, I. H. (2018). Electrospinning of polyethylene terephthalate (PET) nanofibers: optimization study using taguchi design of experiment. *IOP Conference Series Materials Science and Engineering, 454*, 012130. https://doi.org/10.1088/1757-

899x/454/1/012130

Asada, C., Kita, A., Sasaki, C., & Nakamura, Y. (2011). Ethanol production from disposable aspen chopsticks using delignification pretreatments. *Carbohydrate Polymers, 85*(1), 196–200. https://doi.org/10.1016/j.carbpol.2011.02.020

Bennett, A., & Bogorad, L. (1973). Complementary chromatic adaptation in a filamentous blue-green alga. The Journal of Cell Biology, 58(2), 419–435. https://doi.org/10.1083/jcb.58.2.419.

Bösiger, P., Richard, I. M. T., Le Gat, L., Michen, B., Schubert, M., Rossi, R. M., & Fortunato, G. (2018). Application of response surface methodology to tailor the surface chemistry of electrospun chitosan-poly(ethylene oxide) fibers. *Carbohydrate Polymers, 186*, 122–131. https://doi.org/10.1016/j.carbpol.2018.01.038

Bülbül, E. Ö., Okur, M. E., Okur, N. Ü., & Siafaka, P. I. (2022). Traditional and advanced wound dressings: physical characterization and desirable properties for wound healing. In *Elsevier eBooks* (pp. 19–50). https://doi.org/10.1016/b978-0-323-90514-5.00020-1

Buliga, D., Mocanu, A., Rusen, E., Diacon, A., Toader, G., Brincoveanu, O., Călinescu, I., & Boscornea, A. C. (2024). Phycocyanin-Loaded Alginate-Based Hydrogel Synthesis and Characterization. *Marine Drugs, 22*(10), 434. https://doi.org/10.3390/md22100434

Chandra, J. C. S., George, N., & Narayanankutty, S. K. (2016). Isolation and characterization of cellulose nanofibrils from arecanut husk fibre. *Carbohydrate Polymers, 142*, 158-166. https://doi.org/10.1016/j.carbpol.2016.01.015

Chang, C., Chen, C., Yang, C., Chen, Y., Huang, M., Chang, C., Shie, J., Yuan, M., Chen, Y., Ho, C., Li, K., & Yang, M. (2016). Conversion of waste bamboo chopsticks to bio-oil via catalytic hydrothermal liquefaction using K2CO3. *Sustainable Environment*

Research, 26(6), 262–267. https://doi.org/10.1016/j.serj.2016.08.002

Charoensopa, K., et al. (2024). Extraction of nanocellulose from the residue of sugarcane bagasse fiber for Anti-Staphylococcus aureus (S. aureus) application. Polymers, 16(11), 1612. https://doi.org/10.3390/polym16111612

Chen, K., Hu, H., Zeng, Y., Pan, H., Wang, S., Zhang, Y., Shi, L., Tan, G., Pan, W., & Liu, H. (2022). Recent advances in electrospun nanofibers for wound dressing. European Polymer *Journal, 178*, 111490. https://doi.org/10.1016/j.eurpolymj.2022.111490

Chiang, K., Chen, Y., Tsai, W., Lu, C., & Chien, K. (2012). Effect of calcium based catalyst on production of synthesis gas in gasification of waste bamboo chopsticks. *International Journal of Hydrogen Energy, 37*(18), 13737–13745. https://doi.org/10.1016/j.ijhydene.2012.03.042

Chieng, B., Lee, S., Ibrahim, N., Then, Y., & Loo, Y. (2017). Isolation and Characterization of Cellulose Nanocrystals from Oil Palm Mesocarp Fiber. *Polymers, 9*(8), 355. https://doi.org/10.3390/polym9080355

Couret, L., Irle, M., Belloncle, C., & Cathala, B. (2017). Extraction and characterization of cellulose nanocrystals from post-consumer wood fiberboard waste. *Cellulose, 24*(5), 2125–2137. https://doi.org/10.1007/s10570-017-1252-7

Das, S. K., Chakraborty, S., Naskar, S., & Rajabalaya, R. (2021). Techniques and methods used for the fabrication of bionanocomposites. In *Elsevier eBooks* (pp. 17–43). https://doi.org/10.1016/b978-0-12-821280-6.00007-6

Dranseikienė, D., Balčiūnaitė-Murzienė, G., Karosienė, J., Morudov, D., Juodžiukynienė, N., Hudz, N., Gerbutavičienė, R. J., & Savickienė, N.

(2022). Cyano-Phycocyanin: Mechanisms of action on human skin and future perspectives in medicine. *Plants, 11*(9), 1249. https://doi.org/10.3390/plants11091249

Duong, T. (2020). Some statistical techniques applied to engineering mechanics problems. *Vietnam Journal of Science and Technology. 57*. 10. 10.15625/2525-2518/57/6A/14006

Fraley, S., Zalewski, J., Oom, M., & Terrien, B. (2023, March 11). 14.1: *Design of Experiments via Taguchi Methods - Orthogonal Arrays*. Engineering LibreTexts. https://eng.libretexts.org/Bookshelves/Industrial_and_Systems_Engineering/Chemical_Process_Dynamics_and_Controls_(Woolf)/14%3A_Design_of_Experiments/14.01%3A_Design_of_Experiments_via_Taguchi_Methods_-_Orthogonal_Arrays

Gao, M., Yang, Z., Liang, W., Ao, T., & Chen, W. (2023). Recent advanced freestanding pseudocapacitive electrodes for efficient capacitive deionization. *Separation and Purification Technology, 324*, 124577. https://doi.org/10.1016/j.seppur.2023.124577

Garcia, J., et al. (2022). Effect of solvent and additives on the electrospinnability of BSA solutions. Colloids and Surfaces B Biointerfaces, 217, 112683. https://doi.org/10.1016/j.colsurfb.2022.112683

Gefen, A. (2021). *The role of the thermal conductivity of dressings in prevention and treatment of wounds*. Wounds International, 12(1), 18–24. https://woundsinternational.com/wp-content/uploads/2023/02/a0ce5d0a6b4faaaa7d441791c8fdb544.pdf

Haider, A., et al. (2018). A comprehensive review summarizing the effect of electrospinning parameters and potential applications of nanofibers in biomedical and biotechnology. Arabian Journal of Chemistry, 11(8), 1165–1188.

https://doi.org/10.1016/j.arabjc.2015.11.015

Hajieghrary, F., Ghanbarzadeh, B., Pezeshki, A., Dadashi, S., & Falcone, P. M. (2024). Development of hybrid Electrospun Nanofibers: Improving effects of cellulose nanofibers (CNFs) on electrospinnability of gelatin. *Foods, 13*(13), 2114. https://doi.org/10.3390/foods13132114

Hamzaçebi, C. (2020). Taguchi method as a robust design tool. In *IntechOpen eBooks*. https://doi.org/10.5772/intechopen.94908

Huang, S., Zhou, L., Li, M., Wu, Q., & Zhou, D. (2017). Cellulose nanocrystals (CNCs) from corn stalk: Activation energy analysis. Materials, 10(1), 80. https://doi.org/10.3390/ma10010080

Irmak, N. Ş. O. (2020). Taguchi's design for optimization of phycocyanin extraction from Arthrospira (Spirulina) platensis. *GSC Biological and Pharmaceutical Sciences, 11*(3), 006–013. https://doi.org/10.30574/gscbps.2020.11.3.0158

Isogai, A. (2013). Wood nanocelluloses: fundamentals and applications as new bio-based nanomaterials. *Journal of Wood Science, 59*(6), 449–459. https://doi.org/10.1007/s10086-013-1365-z

Jelle, B. P., Rüther, P., & Hovde, P. J. (2012). Investigations of Accelerated Climate Aged wood Substrates by Fourier Transform Infrared Material Characterization. *Advances in Materials Science and Engineering, 2012*, 1–6. https://doi.org/10.1155/2012/827471

Ji, X., Guo, J., Guan, F., Liu, Y., Yang, Q., Zhang, X., & Xu, Y. (2021). Preparation of electrospun polyvinyl Alcohol/Nanocellulose composite film and evaluation of its biomedical performance. *Gels, 7*(4), 223. https://doi.org/10.3390/gels7040223

Jiyas, N., Sasidharan, I., & Kumar, K. B. (2023). Tensile properties and morphological insights into chemically modified fibres

of Pseudoxytenanthera bamboo species as sustainable reinforcements in composites. *Advances in Bamboo Science, 5*, 100050. https://doi.org/10.1016/j.bamboo.2023.100050

Kandala, A. V. U., Solomon, D. G., & Arulraj, J. J. (2022). Advantages of Taguchi method compared to response surface methodology for achieving the best surface finish in wire electrical discharge machining (WEDM). *Journal of Mechanical Engineering, 19*(1), 185-199. https://myjurnal.mohe.gov.my/public/article-view.php?id=181178

Karazi, S. M., Moradi, M., & Benyounis, K. Y. (2019). Statistical and Numerical Approaches for modeling and optimizing laser micromachining Process-Review. In *Elsevier eBooks*. https://doi.org/10.1016/b978-0-12-803581-8.11650-9

Kargarzadeh, H., Huang, J., Lin, N., Ahmad, I., Mariano, M., Dufresne, A., Thomas, S., & Gałęski, A. (2018). Recent developments in nanocellulose-based biodegradable polymers, thermoplastic polymers, and porous nanocomposites. *Progress in Polymer Science, 87*, 197–227. https://doi.org/10.1016/j.progpolymsci.2018.07.008

Kaur, P., Sharma, N., Munagala, M., Rajkhowa, R., Aallardyce, B., Shastri, Y., & Agrawal, R. (2021). Nanocellulose: Resources, Physio-Chemical properties, current uses and future applications. *Frontiers in Nanotechnology, 3*. https://doi.org/10.3389/fnano.2021.747329

Khandual, S., Sanchez, E. O. L., Andrews, H. E., & De La Rosa, J. D. P. (2021). Phycocyanin content and nutritional profile of Arthrospira platensis from Mexico: efficient extraction process and stability evaluation of phycocyanin. *BMC Chemistry, 15*(1). https://doi.org/10.1186/s13065-021-00746-1

Kharazmi, A., Faraji, N., Hussin, R. M., Saion, E., Yunus, W. M. M., & Behzad, K. (2015). Structural, optical, opto-thermal and thermal properties of ZnS–PVA nanofluids synthesized through a radiolytic approach. *Beilstein Journal of Nanotechnology, 6*, 529–536. https://doi.org/10.3762/bjnano.6.55

Kim, K. D., Han, D. N., & Kim, H. T. (2004). Optimization of experimental conditions based on the Taguchi robust design for the formation of nano-sized silver particles by chemical reduction method. *Chemical Engineering Journal, 104*(1–3), 55–61. https://doi.org/10.1016/j.cej.2004.08.003

Kondor, A., Santmarti, A., Mautner, A., Williams, D., Bismarck, A., & Lee, K. (2021). On the BET surface area of nanocellulose determined using volumetric, gravimetric and chromatographic adsorption methods. Frontiers in Chemical Engineering, 3. https://doi.org/10.3389/fceng.2021.738995

Krishna, P. S., Sudha, S., Reddy, K. A., Al-Dhabaan, F. A., Meher, N., Prakasham, R., & Charya, M. S. (2017). Studies on wound healing potential of red pigment isolated from marine Bacterium Vibrio sp. *Saudi Journal of Biological Sciences, 26*(4), 723–729. https://doi.org/10.1016/j.sjbs.2017.11.035

Kumar, P., Miller, K., Kermanshahi-Pour, A., Brar, S. K., Beims, R. F., & Xu, C. C. (2022). Nanocrystalline cellulose derived from spruce wood: Influence of process parameters. *International Journal of Biological Macromolecules, 221,* 426–434. https://doi.org/10.1016/j.ijbiomac.2022.09.017

Lee, H., Yamaguchi, K., Nagaishi, T., Murai, M., Kim, M., Wei, K., Zhang, K., & Kim, I. S. (2017). Enhancement of mechanical properties of polymeric nanofibers by controlling crystallization behavior using a simple freezing/thawing process. *RSC Advances, 7*(69), 43994–44000. https://doi.org/10.1039/c7ra06545k

Leonés, A., Salaris, V., Mujica-Garcia, A., Arrieta, M. P., Lopez, D., Lieblich, M., Kenny, J. M.,

& Peponi, L. (2021). PLA Electrospun Fibers Reinforced with Organic and Inorganic Nanoparticles: A Comparative Study. *Molecules, 26*(16), 4925. https://doi.org/10.3390/molecules26164925

Li, N., Shi, C., Zhang, Z., Wang, H., & Liu, Y. (2019). A review on mixture design methods for geopolymer concrete. *Composites Part B: Engineering, 178*, 107490. https://doi.org/10.1016/j.compositesb.2019.107490

Liao, J., Nie, J., Sun, B., Jiao, T., Zhang, M., & Song, S. (2024). A cellulose composite filter with multi-stage pores had high filtration efficiency, low pressure drop, and degradable properties. *Chemical Engineering Journal, 482*, 148908. https://doi.org/10.1016/j.cej.2024.148908

Liao, H., Wu, Y., Wu, M., Zhan, X., & Liu, H. (2011). Aligned electrospun cellulose fibers reinforced epoxy resin composite films with high visible light transmittance. *Cellulose, 19*(1), 111–119. https://doi.org/10.1007/s10570-011-9604-1

Lin, K., Enomae, T., & Chang, F. (2019). Cellulose Nanocrystal Isolation from Hardwood Pulp using Various Hydrolysis Conditions. *Molecules, 24*(20), 3724. https://doi.org/10.3390/molecules24203724

Luraghi, A., Peri, F., & Moroni, L. (2021). Electrospinning for drug delivery applications: A review. *Journal of Controlled Release, 334*, 463-484. https://doi.org/10.1016/j.jconrel.2021.03.033

Martins, R., Mouro, C., Pontes, R., Nunes, J., & Gouveia, I. (2023). Natural Deep Eutectic Solvent Extraction of Bioactive Pigments from Spirulina platensis and Electrospinning Ability Assessment. *Polymers, 15*(6), 1574. https://doi.org/10.3390/polym15061574

Meng, Y., Wang, X., Wu, Z., Wang, S., & Young, T. M. (2015). Optimization of cellulose nanofibrils carbon aerogel fabrication using response surface methodology. *European Polymer Journal, 73*, 137–148. https://doi.org/10.1016/j.eurpolymj.2015.10.007

Mishra, R. K., Ha, S. K., Verma, K., & Tiwari, S. K. (2018). Recent progress in selected bio-nanomaterials and their engineering applications: An overview. Journal of Science: Advanced *Materials and Devices, 3*(3), 263-288. https://doi.org/10.1016/j.jsamd.2018.05.003

Mohammadi, M., Mohammadi, N., & Mehdipour-Ataei, S. (2020). On the preparation of thin nanofibers of polysulfone polyelectrolyte for improving conductivity of proton-exchange membranes by electrospinning: Taguchi design, response surface methodology, and genetic algorithm. *International Journal of Hydrogen Energy, 45*(58), 34110–34124. https://doi.org/10.1016/j.ijhydene.2020.09.125

Muraleedharan, M. N., Karnaouri, A., Piatkova, M., Ruiz-Caldas, M., Matsakas, L., Liu, B., Rova, U., Christakopoulos, P., & Mathew, A. P. (2021). Isolation and modification of nano-scale cellulose from organosolv-treated birch through the synergistic activity of LPMO and endoglucanases. *International Journal of Biological Macromolecules, 183*, 101–109. https://doi.org/10.1016/j.ijbiomac.2021.04.136

Novareza, O., Tama, I. P., Setyanto, N. W., Kusuma, L., Nirmalasari, P. C. (2017). APPLICATION OF TAGUCHI EXPERIMENT FOR THE COMPOSITION OPTIMIZATION OF RAW MATERIAL IN MAKING OF TERRAZO CHAIR. *Journal of Environmental Engineering and Sustainable Technology, 4*(2), 103-110. doi:http://dx.doi.org/10.21776/ub.jeest.2017.004.02.6

O'Connor, R., Cahill, P., & McGuinness, G. (2021). Effect of electrospinning parameters on the mechanical and morphological characteristics of small diameter PCL tissue engineered blood vessel scaffolds having distinct micro

and nano fibre populations – A DOE approach. *Polymer Testing, 96*, 107119. https://doi.org/10.1016/j.polymertesting.2021.107119

Oon, S. (2022). *The environmental impact of disposable chopsticks*. FoodUnfolded. https://www.foodunfolded.com/article/the-environmental-impact-of-disposable-chopsticks

Pai, C., Boyce, M. C., & Rutledge, G. C. (2009). Morphology of Porous and Wrinkled Fibers of Polystyrene Electrospun from Dimethylformamide. *Macromolecules, 42*(6), 2102–2114. https://doi.org/10.1021/ma802529h

Patel, D. K., Dutta, S. D., Hexiu, J., Ganguly, K., & Lim, K.-T. (2020). Bioactive electrospun nanocomposite scaffolds of poly(lactic acid)/cellulose nanocrystals for bone tissue engineering. *International Journal of Biological Macromolecules, 162*, 1429–1441. https://doi.org/10.1016/j.ijbiomac.2020.07.246

Paulett, K., Brayer, W. A., Hatch, K., Kalous, T., Sewell, J., Liavitskaya, T., Vyazovkin, S., Liu, F., Lukáš, D., & Stanishevsky, A. (2017). Effect of nanocrystalline cellulose addition on needleless alternating current electrospinning and properties of nanofibrous polyacrylonitrile meshes. *Journal of Applied Polymer Science, 135*(5). https://doi.org/10.1002/app.45772

Pauly, H. M., Kelly, D. J., Popat, K. C., Trujillo, N. A., Dunne, N. J., McCarthy, H. O., & Donahue, T. L. H. (2016). Mechanical properties and cellular response of novel electrospun nanofibers for ligament tissue engineering: Effects of orientation and geometry. *Journal of the Mechanical Behavior of Biomedical Materials/Journal of Mechanical Behavior of Biomedical Materials, 61*, 258–270. https://doi.org/10.1016/j.jmbbm.2016.03.022

Raju, V., Revathiswaran, R., Subramanian, K. S., Parthiban, K. T., Chandrakumar, K., Anoop, E. V., & Chirayil, C. J. (2023). Isolation and characterization of nanocellulose from selected hardwoods, viz.,

Eucalyptus tereticornis Sm. and Casuarina equisetifolia L., by steam explosion method. *Scientific Reports, 13*(1). https://doi.org/10.1038/s41598-022-26600-5

Ribeiro, A. S., Costa, S. M., Ferreira, D. P., Calhelha, R. C., Barros, L., Stojković, D., Soković, M., Ferreira, I. C., & Fangueiro, R. (2021). Chitosan/nanocellulose electrospun fibers with enhanced antibacterial and antifungal activity for wound dressing applications. *Reactive and Functional Polymers/Reactive & Functional Polymers, 159*, 104808. https://doi.org/10.1016/j.reactfunctpolym.2020.104808

Saraswat, P., Singh, S., Prasad, M., Misra, R., Rajput, V. D., & Ranjan, R. (2023). Applications of bio-based nanomaterials in environment and agriculture: A review on recent progresses. *Hybrid Advances, 4*, 100097. https://doi.org/10.1016/j.hybadv.2023.100097

Shanmugam, A., Sigamani, S., Venkatachalam, H., Jayaraman, J., & Ramamurthy, D. (2017). Antibacterial activity of extracted phycocyanin from Oscillatoria sp. *Journal of Applied Pharmaceutical Science, 7*(3), 62-67. https://doi.org/10.7324/japs.2017.70310

Sihag, S. S., Pal, J., & Yadav, M. (2022). Extraction and Characterization of Nanocellulose from Wheat Straw: Facile Approach. *Journal of Water and Environmental Nanotechnology, 7*(3), 317-331. https://doi.org/10.22090/jwent.2022.03.007

Singh, H., Verma, A. K., Trivedi, A. K., & Gupta, M. (2023). Characterization of nanocellulose isolated from bamboo fibers. *Materials Today: Proceedings.* https://doi.org/10.1016/j.matpr.2023.02.300

Sulaiman, O., Ghani, N. S., Rafatullah, M., Hashim, R., & Ahmad, A. (2011). Sorption Equilibrium and Thermodynamic Studies of Zinc (II) Ions from Aqueous Solutions by Bamboo Sawdust. *Journal of Dispersion Science and Technology, 32*(4), 583–590.

https://doi.org/10.1080/0193269100 3757322

Sun, Y., Cheng, S., Lu, W., Wang, Y., Zhang, P., & Yao, Q. (2019). Electrospun fibers and their application in drug controlled release, biological dressings, tissue repair, and enzyme immobilization. *RSC Advances, 9*(44), 25712–25729. https://doi.org/10.1039/c9ra05012d

Suzuki, A., Sasaki, C., Asada, C., & Nakamura, Y. (2018). Production of cellulose nanofibers from Aspen and Bode chopsticks using a high temperature and high pressure steam treatment combined with milling. *Carbohydrate Polymers, 194*, 303–310. https://doi.org/10.1016/j.carbpol.2018.04.047

Trushina, D. B., Borodina, T. N., Belyakov, S., & Antipina, M. N. (2022). Calcium carbonate vaterite particles for drug delivery: Advances and challenges. *Materials Today Advances, 14*, 100214. https://doi.org/10.1016/j.mtadv.2022 .100214

Valizadeh, A., & Farkhani, S. M. (2013). Electrospinning and electrospun nanofibres. *IET Nanobiotechnology, 8*(2), 83–92. https://doi.org/10.1049/iet-nbt.2012.0040

Velázquez, M. E., et al. (2022). Nanocellulose extracted from Paraguayan residual agro-industrial biomass: Extraction process, physicochemical and morphological characterization. Sustainability, 14(18), 11386. https://doi.org/10.3390/su14181138 6

Vishnoi, Y., Trivedi, A. K., Gupta, M., Singh, H., Rangappa, S. M., & Siengchin, S. (2023). Extraction of nano-crystalline cellulose for development of aerogel: Structural, morphological and antibacterial analysis. *Heliyon, 10*(1), e23846. https://doi.org/10.1016/j.heliyon.2023.e23846

Wahib, S. A., Da'na, D. A., & Al-Ghouti, M. A. (2022). Insight into the extraction and characterization of cellulose nanocrystals from date pits. *Arabian Journal of Chemistry, 15*(3), 103650.

https://doi.org/10.1016/j.arabjc.2021 .103650

Wang, D., Cheng, W., Yue, Y., Xuan, L., Ni, X., & Han, G. (2018). Electrospun Cellulose Nanocrystals/Chitosan/Polyvinyl Alcohol Nanofibrous Films and their Exploration to Metal Ions Adsorption. *Polymers, 10*(10), 1046. https://doi.org/10.3390/polym10101 046

Wang, T., & Zhao, Y. (2020). Optimization of bleaching process for cellulose extraction from apple and kale pomace and evaluation of their potentials as film forming materials. *Carbohydrate Polymers, 253*, 117225. https://doi.org/10.1016/j.carbpol.2020.117225

Wang, X., Cheng, W., Wang, D., Ni, X., & Han, G. (2019). Electrospun polyvinylidene fluoride-based fibrous nanocomposite membranes reinforced by cellulose nanocrystals for efficient separation of water-in-oil emulsions. *Journal of Membrane Science, 575*, 71–79. https://doi.org/10.1016/j.memsci.2018.12.057

Wulandari, W. T., Rochliadi, A., & Arcana, I. M. (2016). Nanocellulose prepared by acid hydrolysis of isolated cellulose from sugarcane bagasse. *IOP Conference Series Materials Science and Engineering, 107*, 012045. https://doi.org/10.1088/1757-899x/107/1/012045

Xu, W., Xin, B., & Yang, X. (2020). Carbonization of electrospun polyacrylonitrile (PAN)/cellulose nanofibril (CNF) hybrid membranes and its mechanism. *Cellulose, 27*(7), 3789–3804. https://doi.org/10.1007/s10570-020-03006-y

Xu, Y., Wu, Z., Li, A., Chen, N., Rao, J., & Zeng, Q. (2024). Nanocellulose composite films in food packaging materials: a review. *Polymers, 16*(3), 423. https://doi.org/10.3390/polym16030 423

Zarina, S., & Ahmad, I. (2014). Biodegradable Composite Films based on κ-carragee-

nan Reinforced by Cellulose Nanocrystal from Kenaf Fibers. *BioResources, 10*(1). https://doi.org/10.15376/biores.10.1.256-271

Zhang, H., Fu, S., & Chen, Y. (2020). Basic understanding of the color distinction of lignin and the proper selection of lignin in color-depended utilizations. *International Journal of Biological Macromolecules, 147*, 607–615. https://doi.org/10.1016/j.ijbiomac.2020.01.105

Zhang, H., Zhang, F., & Huang, Q. (2017). Highly effective removal of malachite green from aqueous solution by hydrochar derived from phycocyanin-extracted algal bloom residues through hydrothermal carbonization. *RSC Advances, 7*(10), 5790–5799. https://doi.org/10.1039/c6ra27782a

Zhang, Q., Young, T. M., Harper, D. P., Liles, T., & Wang, S. (2021). Optimization of electrospun poly(vinyl alcohol)/cellulose nanocrystals composite nanofibrous filter fabrication using response surface methodology. *Carbohydrate Polymer Technologies and Applications, 2*, 100120. https://doi.org/10.1016/j.carpta.2021.100120

Zhang, Y., Zhang, C., & Wang, Y. (2021). Recent progress in cellulose-based electrospun nanofibers as multifunctional materials. *Nanoscale Advances, 3*(21), 6040–6047. https://doi.org/10.1039/d1na00508a